High-harmonic-generation-inspired preparation of optical vortex arrays with arbitrary-order topological charges

Wuhong Zhang (张武虹) and Lixiang Chen (陈理想)*

Department of Physics, College of Physics Science and Technology, Xiamen University, Xiamen 361005, China
**Corresponding author: chenlx@xmu.edu.cn*

Received November 5, 2017; accepted January 12, 2018; posted online March 6, 2018

In the process of high-harmonic generation with a Laguerre-Gaussian (LG) mode, it was well established that the topological charge could be of an N-fold increase due to angular momentum conservation. Here, by mimicking the effect of high-harmonic generation, we devise a simple algorithm to generate optical vortex arrays carrying arbitrary topological charges with a single phase-only spatial light modulator. By initially preparing a coaxial superposition of suitable low-order LG modes, we demonstrate experimentally that the topological charges of the embedded vortices can be multiplied and transformed into arbitrarily high orders on demand, while the array structure remains unchanged. Our algorithm offers a concise way to efficiently manipulate the structured light beams and holds promise in optical micromanipulation and remote sensing.

OCIS codes: 050.4865, 070.6120, 140.3300, 090.1995.
doi: 10.3788/COL201816.030501.

An optical vortex possesses a phase singularity, and the optical energy flows around the singular point. The optical vortex is also connected to the orbital angular momentum (OAM) of light, whose helical phasefront is described by $\exp(i\ell\phi)$, where ϕ is the azimuthal angle, and $\ell\hbar$ is the OAM carried per photon[1]. Generally, the topological charge of a vortex filed is defined as $Q = (2\pi)^{-1}\oint_C \mathrm{d}\chi$, where χ describes the phase distribution, and C is an arbitrary circuit enclosing the singular point[2]. The optical vortices as well as light's OAM have been extensively explored for a variety of interesting applications, including optical tweezers and spanners[3], spatial mode multiplexing in optical communications[4], optical sensing[5] and metrology[6], and high-dimensional quantum information protocols[7]. Besides, the OAM content of an optical vortex array[8] and the nonlinear propagation of an array of singularities were investigated[9]. Also, optical vortex arrays have been applied to assembling fluid-borne colloidal spheres into rapidly circulating rings so that the generating fluid flows with pinpoint control[10]. More recently, we also demonstrated a high-efficiency scheme of detecting the arrayed optical vortices even hidden in an ultra-weak background[11].

As a reliable method to generate optical vortex arrays, the computer-generated holograms, acting as diffractive optical elements, have been widely used in dynamic holographic optical tweezers[12]. A single collimated laser beam can be easily split into several separated beams with optical vortices by utilizing a spatial light modulator (SLM)[13,14]. Besides, some other special instrumentation can also be used to produce optical vortex arrays, for example, a thin-slice solid-state laser[15], a $\pi/2$ cylindrical lens mode converter[16], a mode selective coupler[17], and a single topological defect in a nematic liquid crystal mesophase[18]. By interfering with three or more plane or spherical waves, it is demonstrated that the vortex arrays can be easily produced and controlled[19–21]. Based on the coaxial superposition of Laguerre-Gaussian (LG) modes instead of plane waves, interesting structures of optical singularities are also reported[22], and its diffraction theory is also analyzed[23].

However, the topological charges of a vortex array produced by the interference scheme are generally of low orders, and the LG mode coaxial superposition method has not been fully exploited[19–22]. Here, we use suitable LG mode superposition as the initial optical vortex arrays, and then we devise a simple yet effective mathematical algorithm that can multiply these vortices into arbitrary orders, while the array structure remains unchanged. Our approach is inspired by the nonlinear optical effect of high-harmonic generation, where the topological charge of an input LG mode is multiplied spontaneously due to angular momentum conservation. Besides, the algorithm also provides a quantitative way to define the component and coefficient of each LG mode involved in the formation of vortex arrays, such that one may directly use an LG beam laser instead of using the SLM to produce high-power optical vortex arrays on demand. We emphasize that in this Letter we just mimic this nonlinear optical effect in mathematics to devise and show our algorithm rather than using the real crystal to perform the N-order harmonic generation effect. In our experiment demonstration, the desired holographic gratings loaded in a single phase-only SLM can be utilized to produce vortex arrays carrying tunable high-order topological charges on demand. We generate vortex arrays of triangle, circular, and chessboard structures that carry high-order topological charges to demonstrate the validity of the algorithm. We anticipate that our scheme may find direct applications in the realm of optical micromanipulation.

As a natural choice for describing an optical vortex carrying OAM, an LG mode can be written mathematically in the cylindrical coordinate (ρ, φ) at the beam waist plane as

$$\mathrm{LG}_p^{\ell}(\rho, \phi) = R_p^{\ell}(\rho) \exp(i\ell\phi), \tag{1}$$

and

$$R_p^{\ell}(\rho) = A_{p,\ell}\left(\frac{\sqrt{2}\rho}{\omega}\right)^{|\ell|} \exp\left(\frac{-\rho^2}{\omega^2}\right) L_p^{|\ell|}\left(\frac{2\rho^2}{\omega^2}\right), \tag{2}$$

where ω is the beam waist, $A_{p,\ell}$ is the normalized constant, $L_p^{|\ell|}(\bullet)$ is the generalized Laguerre polynomial, and $R_p^{\ell}(\rho)$ describes the radial intensity distribution, while $\exp(i\ell\phi)$ denotes the helical phase structure with p and ℓ being the radial and azimuthal mode indices, respectively. In the process of high-harmonic generation, we assume the input fundamental wave is an optical vortex beam, $E_1(\rho, \phi) = A_1(\rho)\exp(i\ell\phi)$. Under both slowly varying envelope approximation and small signal approximation, we know the output N-order high-harmonic wave could be described by[24]

$$E_N(\rho, \phi) = \eta[E_1(\rho, \phi)]^N = \eta A_1^N(\rho)\exp(iN\ell\phi), \tag{3}$$

where η is a constant related to the conversion efficiency in the high-harmonic process. Besides, one can see clearly that the topological charge is multiplied, having an N-fold increase, as a consequence of the law of angular momentum conservation. A more simple and intuitive example is the second-harmonic generation (SHG), in which an LG mode of an azimuthal index ℓ will end up with a doubled frequency and a doubled topological charge 2ℓ[25,26]. Recently, an interesting interference phenomenon was also observed in SHG, where a specific superposition of two LG modes of opposite signs served as the input fundamental wave instead of a single LG mode[27,28]. In this case, the resultant SHG light field can be described as $E_2(\rho, \phi) = \eta[\mathrm{LG}_p^{+\ell}(\rho, \phi) + \mathrm{LG}_p^{-\ell}(\rho, \phi)]^2$. Along this line, we can put Eq. (3) in a more general framework with the input light field being an arbitrary superposition of different LG modes, namely,

$$E_N(\rho, \phi) = \left[\sum_{\ell,p} a_{\ell,p}\mathrm{LG}_p^{\ell}(\rho, \phi)\right]^N, \tag{4}$$

where $a_{\ell,p}$ denotes the complex amplitude of the constituent LG modes, and η is trivially discarded. As is inspired by Eq. (4), here we mimic the high-harmonic-generation mechanism to devise an algorithm to prepare optical vortex arrays carrying arbitrarily high-order topological charges with a single SLM. The incident light beams on the SLM are merely fundamental Gaussian ones. Based on the phase holograms prepared by our mathematical codes, we can use the SLM to tune the topological charges of the vortices embedded in a static array. Our algorithm is illustrated by Fig. 1(a). We restrict our attention to those superposition LG modes with $p = 0$, namely, those modes with a single bright annular ring and on-axis zero intensity.

According to the previous study[22], the original light fields $E_1(\rho, \phi)$ in the form of a vortex array carrying low-order topological charges can be produced by superposing a set of suitable LG modes, namely, $E_1(\rho, \phi) = \sum_{\ell} a_{\ell}\mathrm{LG}_{p=0}^{\ell}(\rho, \phi)$. Mathematically, we are allowed to rewrite the vortex field as $E_1(\rho, \phi) = |E_1(\rho, \phi)|\exp[i\chi(\rho, \phi)]$, which can be equivalently represented by an intensity matrix $|E_1(\rho, \phi)|$ and a phase matrix $\chi(\rho, \phi)$. In order to make distinct vortices in the bright background, we only extract the information of the phase matrix and replace the intensity matrix by a uniform intensity. Under this configuration and based on Eq. (3), we know that the resultant vortex field will become $E_N(\rho, \phi) \propto \exp[iN\chi(\rho, \phi)]$. Then, the topological charge of each vortex embedded in the light field will be increased by N times as $Q' = (2\pi)^{-1}\oint_C \mathrm{d}(N\chi) = NQ$. Then, we add the phase profile to the blazing grating and obtain the desired holograms that are displayed subsequently on the SLM. This is different from the previous work of preparing single high-order OAM beams, since it just uses single LG modes and cannot generate the high-order vortex arrays of various interesting structures[29]. To illustrate our algorithm more clearly, we take the superposition of three LG modes, $\ell_1 = 1$, $\ell_2 = 5$, and $\ell_3 = 15$, each with the weight amplitude $a_{\ell_1} = 0.7$, $a_{\ell_2} = 1.1$, and $a_{\ell_3} = 1.5$, for example, to do the numerical simulation. The phase distribution of the original light field is shown in Fig. 1(b). It can be seen that all of the topological charges have the unit topological charge $Q = 1$. Here, without losing generality, we take $N = 3$ to mimic the effect of third-harmonic generation and generate the high-order vortex array with each vortex carrying a topological charge $Q' = 3$, as manifested by the

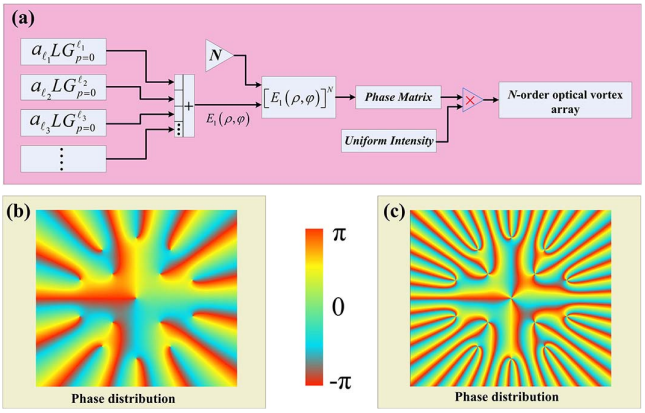

Fig. 1. (a) Schematic illustration of the algorithm: We use specific supposition of low-order LG modes to form the initial optical vortex array fields, $E_1(\rho, \phi)$, then multiply this field by N times. By extracting the phase matrices and imparting a uniform intensity, we then obtain the N-order vortex array efficiently. (b) Simulation of an original optical vortex array field produced by superposing LG modes of $\ell_1 = 1$, $\ell_2 = 5$, and $\ell_3 = 15$. (c) Simulation of a three-order optical vortex array generated from (b) by setting $N = 3$.

characteristic forks in the phase distribution of Fig. 1(c). Besides, the expansion of Eq. (4) gives a polynomial consisting of different LG modes with a fixed coefficient, indicating that our algorithm also provides a quantitative way that one may directly utilize the diode pumping of solid-state LG beam lasers[30,31] to produce an optical vortex array with arbitrary topological charges at a high-energy level.

Our experimental setup is sketched in Fig. 2. The light source is a linearly polarized fundamental Gaussian mode derived from a 2 mW, 633 nm HeNe laser. After being collimated by a telescope, the light beam is separated into two parts, i.e., the reflected one trivially serves as a reference beam, while the transmitted one is expanded and incident on a computer-controlled SLM (Hamamatsu, X10486-1). The SLM serves as a reflective device consisting of an array of 792 pixel × 600 pixel with an effective area of 16 mm × 12 mm and a pixel pitch of 20 μm. Each pixel imprints individually the incoming light with a phase modulation (0–2π), according to the 8 bit grayscale (0–255). The whole SLM acts as a reconfigurable diffractive element, allowing an interactive manipulation with a response time comparable to the video displays[29,32]. Based on the algorithm shown in Fig. 1(a), we prepare and display the holographic gratings in the SLM. Then, we make the first diffraction order of reflected light propagate through a 4f system consisting of two lenses and an adjustable iris placed at the focal plane. We direct the desired light field of the vortex array to interfere with a tilted reference plane wave at the second beam splitter (BS2). A color CCD camera placed in the image plane is used to record the interference intensity patterns.

According to our algorithm in Fig. 1(a), the first key step is to mathematically prepare the holographic gratings based on the superposition of a set of suitable standard LG modes. For seeking the simplicity but without losing the generality, we first considered the coaxial superposition of two LG modes. For example, we present the experimental results for the unbalanced superposition of $\mathrm{LG}^0_{p=0}$ and $\mathrm{LG}^3_{p=0}$, namely, $E_1(\rho,\phi) = 0.8\mathrm{LG}^0_{p=0}(\rho,\phi) + \mathrm{LG}^3_{p=0}(\rho,\phi)$. From the theoretical simulation of Figs. 3(a) and 3(b), one can see that each vortex in the initial triangular array

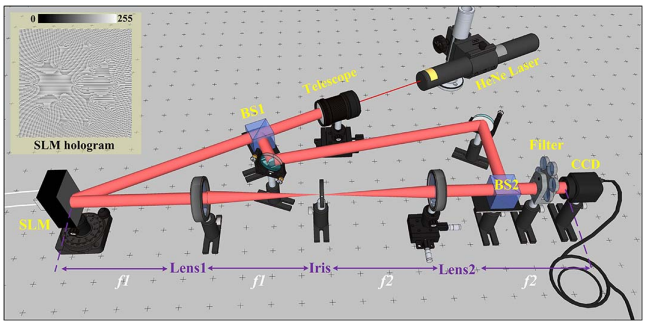

Fig. 2. A schematic overview of the experimental setup to generate vortex arrays carrying high-order topological charges.

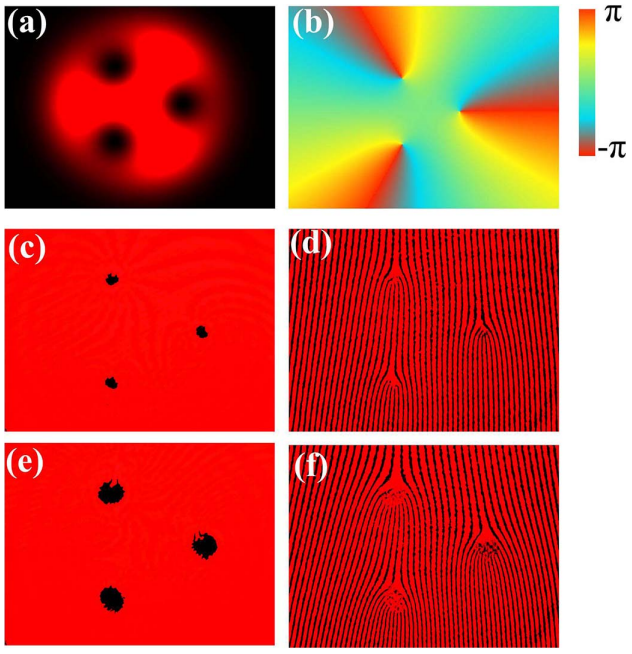

Fig. 3. (a), (b) Simulation results of the intensity and phase distributions of the original optical vortex array field with $0.8\mathrm{LG}^0_0 + \mathrm{LG}^3_0$. (c), (d) The five-order and (e), (f) ten-order optical vortex array fields and their interference fringes with a tilt plane wave.

merely carries one unit topological charge. Based on our algorithm, we extract the phase distribution of $E_1(\rho,\phi)$ and multiply it by N times, such that we obtain the tunable topological charges, while the triangular structure stays unaffected. For example, by simply setting $N = 5$ and 10 in our mathematical codes, we can conveniently obtain the newly generated arrays carrying high-order topological charges $Q' = 5$ and $Q' = 10$, respectively. The intensity of Figs. 3(c) and 3(e) obviously shows that a higher vortex leads to a larger dark hole at its center zone. Besides, we record the interference patterns of Figs. 3(d) and 3(f), where the five-prong and ten-prong forks clearly reveal the topological charges, respectively. In Fig. 4, we further consider another two-mode superposition, $E_1(\rho,\phi) = \mathrm{LG}^5_{p=0}(\rho,\phi) + \mathrm{LG}^{15}_{p=0}(\rho,\phi)$, which initially generates a vortex ring of $Q = 1$ around a vortex center of $Q = 5$. By setting $N = 2$, we can make the ring vortices carry a topological charge $Q' = 2$, while the center vortex $Q' = 10$, see Fig. 4(c). Similarly, we can triple the topological charges of all the vortices located at the ring and center by setting $N = 3$, see Fig. 4(e). The corresponding vortex numbers are also manifested by the characteristic forks after interfering with a tilted plane wave, see Figs. 4(d) and 4(f), respectively.

As the LG modes constitute a set of complete orthogonal bases, it would be interesting to see the coaxial superposition of more than two LG modes. We consider such a case in Fig. 5, where we display the mode superpositions with the OAM spectra. As more LG modes are involved in the formation of the vortex array, we can see that a more

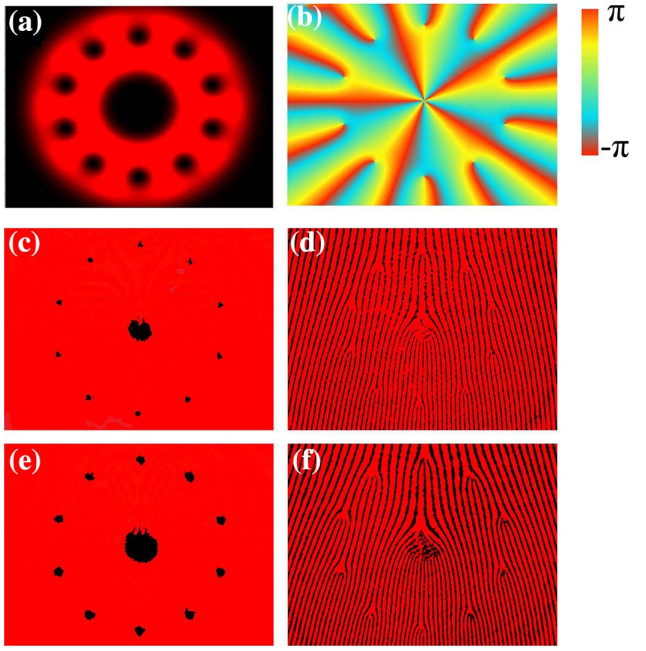

Fig. 4. (a), (b) Simulation results of the intensity and phase distributions of the original optical vortex array field with $LG_0^5 + LG_0^{15}$. (c), (d) The two-order and (e), (f) three-order optical vortex array fields and their interference fringes with a tilt plane wave.

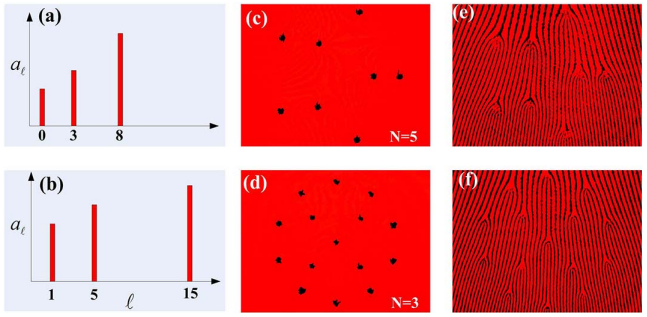

Fig. 5. (a), (b) Theoretical spectra of LG modes involved in producing original optical vortex arrays. (c), (d) Experimental results of corresponding five- and three-order optical vortex arrays. (e), (f) The corresponding interference fringes with a tilt plane wave.

complex structure appears, like the chess pieces spreading over a chessboard, by adjusting the weight coefficient a_ℓ, as shown in Figs. 5(a) and 5(b). Each vortex embedded in the initial light fields carries only a single-unit topological charge. However, based on our algorithm, we obtain the five- and three-order vortex arrays in Figs. 5(c) and 5(d), respectively. The five-prong and three-prong forks of the interference patterns in Figs. 5(e) and 5(f) also reveal clearly the number of the topological charges. Thus, we are allowed to draw a conclusion that if we superpose more LG modes with tunable weight coefficients, it is possible to produce any structured vortex array bearing arbitrarily high-order topological charges.

We have demonstrated a feasible method to produce high-order optical vortex arrays. Mathematically, our method was based on a simple but effective algorithm, which extracts and multiplies the pure phase matrices of an initial low-order vortex array from the simple superposition of suitable LG modes. With the use of a single phase-only SLM, we prepared a variety of optical vortex structures, including the triangular, ring, and chessboard arrays, carrying high-order topological charges. Remarkably, our idea might also be directly implemented with an efficient high-order-harmonic-generation crystal[33]. It is noted that, unlike a strongly focused Gaussian laser, an optical vortex can serve as a novel optical trap, where the trapped particles, such as a biological red blood cell, will not suffer optical damage by absorptive heating[34]. In our scheme, we are able to multiply the topological charges while maintaining the vortex structures. Such a feature may lead to some promising applications in optical micromanipulation, such as optical tweezers with a twist[2], where an array of micro particles with a stationary trapping can be accelerated or decelerated in a fast and controllable way.

We are grateful to the Optics group led by Professor Miles Padgett at University of Glasgow for kind support in LabVIEW codes. This work was supported by the National Natural Science Foundation of China (NSFC) (Nos. 11104233 and 11474238), the Fundamental Research Funds for the Central Universities (No. 20720160040), the Natural Science Foundation of Fujian Province (No. 2015J06002), and the Program for New Century Excellent Talents in University (NCET) (NCET-13-0495).

References

1. L. Allen, M. W. Beijersbergen, R. J. C. Spreeuw, and J. P. Woerdman, Phys. Rev. A **45**, 8185 (1992).
2. J. F. Nye and M. V. Berry, Proc. R. Soc. Lond. A **336**, 165 (1974).
3. M. Padgett and R. Bowman, Nat. Photon. **5**, 343 (2011).
4. J. Wang, Photon. Res. **4**, B14 (2016).
5. G. Milione, T. Wang, J. Han, and L. Bai, Chin. Opt. Lett. **15**, 030012 (2017).
6. W. Wang, T. Yokozeki, R. Ishijima, M. Takeda, and S. G. Hanson, Opt. Express **14**, 10195 (2006).
7. X. L. Wang, X. D. Cai, Z. E. Su, M. C. Chen, D. Wu, L. Li, N. L. Liu, C. Y. Lu, and J. W. Pan, Nature **518**, 516 (2015).
8. J. Courtial, R. Zambrini, M. R. Dennis, and M. Vasnetsov, Opt. Express **14**, 938 (2006).
9. G. H. Kim, J. H. Jeon, Y. C. Noh, K. H. Ko, H. J. Moon, J. H. Lee, and J. S. Chang, Opt. Commun. **147**, 131 (1998).
10. K. Ladavac and D. Grier, Opt. Express **12**, 1144 (2004).
11. W. Zhang, J. Wang, F. Li, L. Chen, and E. Karimi, Laser Photon. Rev. **11**, 1600163 (2017).
12. J. E. Curtis, B. A. Koss, and D. G. Grier, Opt. Commun. **207**, 169 (2002).
13. G. X. Wei, L. L. Lu, and C. S. Guo, Opt. Commun. **282**, 2665 (2009).
14. S. J. Huang, J. Zhang, W. Shao, F. Q. Zhu, and T. Y. Wang, Acta Photon. Sin. **46**, 826002 (2017).
15. K. Otsuka and S. C. Chu, Opt. Lett. **34**, 10 (2009).

16. Y. C. Lin, T. H. Lu, K. F. Huang, and Y. F. Chen, Opt. Express **19**, 10293 (2011).
17. X. Zhang, R. Chen, Y. Zhou, H. Ming, and A. T. Wang, Chin. Opt. Lett. **15**, 030008 (2017).
18. E. Brasselet, Phys. Rev. Lett. **108**, 087801 (2012).
19. J. Masajada and B. Dubik, Opt. Commun. **198**, 21 (2001).
20. S. Vyas and P. Senthilkumaran, Appl. Opt. **46**, 2893 (2007).
21. S. Vyas and P. Senthilkumaran, Appl. Opt. **46**, 7862 (2007).
22. T. Ando, N. Matsumoto, Y. Ohtake, Y. Takiguchi, and T. Inoue, J. Opt. Soc. Am. A **27**, 2602 (2010).
23. W. Zhang, Z. Wu, J. Wang, and L. Chen, Chin. Opt. Lett. **14**, 110501 (2016).
24. R. W. Boyd, *Nonlinear Optics*, 3rd ed. (Academic, 2008).
25. J. Courtial, K. Dholakia, L. Allen, and M. J. Padgett, Phys. Rev. A **56**, 4193 (1997).
26. K. Dholakia, N. B. Simpson, M. J. Padgett, and L. Allen, Phys. Rev. A **54**, R3742 (1996).
27. Y. C. Lin, K. F. Huang, and Y. F. Chen, Laser Phys. **23**, 115405 (2013).
28. Z. Y. Zhou, D. S. Ding, Y. K. Jiang, Y. Li, S. Shi, X. S. Wang, and B. S. Shi, Opt. Express **22**, 20298 (2014).
29. L. Chen, W. Zhang, Q. Lu, and X. Lin, Phys. Rev. A **88**, 053831 (2013).
30. Y. Senatsky, J. F. Bisson, J. Li, A. Shirakawa, M. Thirugnanasambandam, and K. I. Ueda, Opt. Rev. **19**, 201 (2012).
31. Y. F. Chen, C. C. Chang, C. Y. Lee, C. L. Sung, J. C. Tung, K. W. Su, H. C. Liang, W. D. Chen, and G. Zhang, Photon. Res. **5**, 561 (2017).
32. W. Zhang, Q. Qi, J. Zhou, and L. Chen, Phys. Rev. Lett. **112**, 153601 (2014).
33. G. Z. Li, Y. P. Chen, H. W. Jiang, and X. F. Chen, Photon. Res. **3**, 168 (2015).
34. R. Dasgupta, S. Ahlawat, R. S. Verma, and P. K. Gupta, Opt. Express **19**, 7680 (2011).